Validation of Jason-3 tracking modes over French rivers

Sylvain Biancamaria, Thomas Schaedele, Denis Blumstein, Frédéric Frappart, François Boy, Jean-Damien Desjonquères, Claire Pottier, Fabien Blarel, Fernando Niño

Validation of Jason-3 tracking modes over French rivers

Sylvain Biancamaria[1], Thomas Schaedele[1], Denis Blumstein[1,2], Frédéric Frappart[1,3], François Boy[2], Jean-Damien Desjonquères[2,*], Claire Pottier[2], Fabien Blarel[1], Fernando Niño[1]

[1] LEGOS, Université de Toulouse, CNES, CNRS, IRD, UPS - 14 avenue Edouard Belin, 31400 Toulouse, France

Email addresses: sylvain.biancamaria@legos.obs-mip.fr; thomas.schaedele@legos.obs-mip.fr; denis.blumstein@cnes.fr; fabien.blarel@legos.obs-mip.fr; fernando.nino@legos.obs-mip.fr

[2] CNES - 18 avenue Edouard Belin, 31401 Toulouse Cedex, France

Email addresses: francois.boy@cnes.fr; jean-damien.m.desjonqueres@jpl.nasa.gov; claire.pottier@cnes.fr

[3] GET, Université de Toulouse, CNRS, IRD, UPS - 14 avenue Edouard Belin, 31400 Toulouse, France

Email address: frederic.frappart@get.obs-mip.fr

[*] Now at JPL - 4800 Oak Grove Drive, Pasadena, CA 91109, USA

Published in Remote Sensing of Environment, doi:10.1016/j.rse.2018.02.037

Abstract

Satellite nadir radar altimeters have been widely used to measure river and lake surface water elevations. They can now retrieve the elevations of some rivers less than 200 m wide. However, as these satellite missions are primarily designed to observe ocean surface topography, they are not always able to observe continental surfaces. For steep-sided rivers (i.e. in river valleys no more than a few km wide and surrounded by slopes over 50 m high), altimeters tend to observe the top of the surrounding topography rather than the river itself.

The Jason-3 altimetry mission, launched in January 2016, has an alternative instrument operation mode, the so called Open-Loop (OL) or Digital Elevation Model (DEM) tracking mode. This mode is intended to help overcome this issue, by using an on-board DEM. However it was not used in 2016 as the operational mode because of difficulties in defining an accurate on-board global-scale DEM. Mainland France has been chosen to test the OL tracking mode, as water masks and DEMs of sufficient accuracy are available.

Following the launch of Jason-3, Jason-2 (its predecessor) was maintained on the same nominal orbit as its follow-on, for more than 6 months. During this tandem period, data from the first 10 Jason-3 cycles (a Jason-2/-3 cycle corresponds to 10 days) were acquired in the traditional Closed-Loop (CL) tracking mode. Jason-3 data from the last 13 cycles were acquired in OL tracking mode. Jason-2 was always in CL tracking mode. Compared to nearby in situ gages and for river wider than 100 m, Jason-3 water elevation anomalies have a RMSE between 0.20 and 0.30 m for most reaches. Jason-3 performance over narrow rivers is similar to that of Jason-2. In CL tracking mode, Jason-3 altimeter tends to be locked over the surrounding topography more frequently than Jason-2 (due to the specific post-launch Jason-2 altimeter tuning). This study shows that Jason-2 observed 60% of river reaches studied (48 of 86 reaches), whereas Jason-3 in

OL tracking mode was able to measure all river reaches for every cycle. This result clearly highlights the significant advantages of the OL tracking mode for observation of steep-sided rivers. However, further investigations are required to compute an accurate on-board global-scale DEM and to determine those locations where the use of OL tracking mode is or is not appropriate.

Keywords: Jason-3; altimetry; rivers; Open-Loop/DEM tracking mode

1. Introduction

Continental water plays an important role in the Earth's water and energy cycles, and is at the interface between the atmosphere and the ocean. For climate studies, long-term (i.e. multi-decadal) observations of the time variations in lake and river levels are necessary to estimate lake storage variability and river discharges. These data are also essential for water management, as water is a resource that is vital to human societies. This monitoring has traditionally been performed using in situ gage networks, which are usually operated at local or national level. However, viewed from a global perspective, in situ networks are heterogeneous. The total number of gages has been decreasing over recent decades (IAHS Ad Hoc Group on Global Water Data Sets et al., 2001), and their measurements are not always shared publicly, especially in transboundary basins (Gleason and Hamdan, 2017). That's why, satellite data, including water elevation measurements obtained from radar altimeters have been used since the early 90's as an additional observation system (e.g. Birkett, 1995), even if they cannot replace in situ gages, as noted by Fekete et al. (2012).

Since the launch in August 1992 of Topex/Poseidon, developed by NASA (National Aeronautics and Space Administration) and CNES (Centre National d'Études Spatiales), nadir radar altimeters have been widely used to measure ocean surface topography, which was the scientific objective of the mission (e.g. Fu and Cazenave, 2001). However, soon after its launch, the high potential of the altimeter to retrieve river and lake water elevations has been demonstrated by Koblinsky et al. (1993). In the present study, water elevation is defined as the distance from the water surface to a reference surface (an ellipsoid or a geoid). Pioneering studies demonstrated that 24 large lakes (with an area greater than 300 km^2) and 8 large rivers (more than 2 km wide) could be measured accurately with, at best, RMSE (Root Mean Square Error) of around 0.04 m and 0.11 m respectively (Birkett, 1995; 1998). Subsequently, radar altimetry has been increasingly used to monitor inland water bodies (for review see for example Crétaux et al., 2017). The launch of Topex/Poseidon was followed by that of several nadir altimetry satellites: ERS-2 in 1995, GFO in 1998, Jason-1 in 2001, ENVISAT in 2002, Jason-2 in 2008, CryoSat-2 in 2010, SARAL in 2013, Jason-3 in 2016 and Sentinel-3A in 2016. Online databases (G-REALM, https://www.pecad.fas.usda.gov/cropexplorer/global_reservoir/; Hydroweb, http://hydroweb.theia-land.fr; River and Lake database, http://tethys.eaprs.cse.dmu.ac.uk/RiverLake/shared/main; DAHITI, http://dahiti.dgfi.tum.de; HydroSat, http://hydrosat.gis.uni-stuttgart.de/php/index.php) using this series of altimeters have been developed over recent decades to provide freely accessible water elevation time series for selected rivers and lakes. Continuity of measurements is also guaranteed, as many nadir altimetry missions are already scheduled for launch in the near future. These include Sentinel-3B (early 2018), Sentinel-3C and -3D (launch dates currently unknown, as they will provide continuity of observation after Sentinel-3A and -3B), Sentinel-6/Jason-CS A (around 2020), and SWOT

(around 2021; this satellite will carry not only a nadir altimeter, but also a wide swath altimeter). Even where the instrument footprint on the ground is a few kilometres wide, enhancements made to the instruments, especially after ENVISAT and Jason-2, have improved the ability to observe smaller water bodies (width < 500 m) to an extent not previously thought possible (e.g. Santos da Silva et al., 2010; Michailovsky et al., 2012; Baup et al., 2014; Frappart et al., 2015a; Sulistioadi et al., 2015; Biancamaria et al., 2017). The ability of an altimeter to observe a river is dependent on river width, but is determined to an even greater extent by the "surrounding topography, the observation configuration, previous measurements and the instrument design" (Baup et al., 2014; Biancamaria et al., 2017).

Nadir altimeters present some limitations. For instance, they provide elevation measurements only along or close to their track (in the nadir direction or in a quasi-nadir direction) and therefore miss many water bodies (the number of objects overflown depends on the satellite orbit). In addition, altimeters are mainly designed to observe oceans with the best accuracy. They are not optimized for the monitoring of continental surfaces, which could pose a problem with steep-sided rivers. For these rivers, the altimeter might measure the top of the surrounding topography, instead of the river valley. This problem has been extensively described and discussed by Biancamaria et al. (2017). However, in the future, more researchers and water resources managers will be interested in the water elevation of steep-sided rivers and smaller rivers. It is therefore important to address this issue as soon as possible, in order to obtain the longest possible time series in the coming decades, over regions previously unobserved by altimetry. To do so, CNES has developed an alternative instrument operating mode, usually referred to as "Open-Loop" (OL) or Digital Elevation Model tracking mode or DEM tracking mode. It requires the loading of an along-track DEM on board the altimeter. Very few studies

have analysed measurements made for such rivers in this tracking mode, in comparison with the usual “Closed-Loop” (CL) tracking mode (Birkett and Beckley, 2010).

The purposes of this study are: (1) to validate measurements of the newly launched Jason-3 satellite (17 January 2016) for small to medium-sized rivers (between 35 m and 300 m wide) over mainland France and (2) to study whether the Jason-3 alternative instrument operating mode is able to overcome the problem of the measurement of steep-sided rivers and is therefore advantageous. Section 2 of this paper discusses nadir altimetry and its potential issue with steep-sided rivers. Section 3 introduces the study domain and the validation data used (sub-section 3.1), the computation of the Jason-3 on-board DEM over the study domain and the Jason-3 data validation methodology (section 3.2). Section 4 then presents and discusses the results obtained. Finally, some conclusions and perspectives on the use of Jason-3 for the measurement of small to medium-sized rivers, in particular those that are steep-sided, are provided in section 5.

2. Satellite Nadir Radar Altimetry and the issue of steep-sided water bodies

2.1. Surface Elevation retrieval from nadir altimetry

Nadir altimeters provide water elevation measurements at the intersections between satellite ground tracks and rivers (or lakes/reservoirs). These intersections are usually referred to as “virtual stations” (VS). A more detailed description of water surface elevation estimation from nadir altimetry over continents can be found, for example, in Biancamaria et al. (2017) and in Crétaux et al. (2017). For this reason, essential information only is mentioned in this section.

Nadir altimeters emit a radar pulse in the nadir direction (or local vertical, Figure 1) and then record the radar echo using a pulse compression technique. This record, also known as the waveform, contains the value of the returned power as a function of time or, equivalently, of

distance between the radar and the reflectors (Chelton et al., 2001; Frappart et al., 2017). The two-way travel time (T), given by the leading edge of the waveform signal, is estimated accurately using a "retracking" algorithm applied to the waveforms by the mission processing centre. This processing is based on the use of a theoretical model built for ocean conditions (Brown, 1977) and provides a high level of precision and accuracy over oceans. Over inland waters, estimation of the two-way travel time is more difficult since the waveform shape, affected by several complex backscattering phenomena, differs markedly from the theoretical model. For these cases, alternative retracking algorithms should be used (e.g. Frappart et al., 2006). The two-way travel time T is converted to the distance between the satellite centre of mass and the ground surface, called the altimeter "range" (R, Figure 1), assuming a constant electromagnetic wave propagation speed equal to the speed of light in vacuum. However, estimates of the range R need to be corrected for propagation delays of the radar signal within the atmosphere (these corrections are labelled $\Delta R_{propagation}$) and for some known geophysical signals that affect measurement (these corrections are labelled $\Delta R_{geophysical}$) (e.g. Chelton et al., 2001; Frappart et al., 2017). In our study, $\Delta R_{propagation}$ includes the ionosphere correction, the dry troposphere correction, and the wet troposphere correction (for more details, see Biancamaria et al., 2017). $\Delta R_{geophysical}$ corresponds to corrections for crustal vertical motions due to the solid Earth and pole tides. Moreover, the satellite altitude (H, Figure 1) can be calculated with an accuracy better than 0.02 m (e.g. Couhert et al., 2015). All these computations allow for the estimation of the ground elevation above the reference ellipsoid (h) from the nadir altimeter, as follows:

$$h = H - \left(R + \Delta R_{propagation} + \Delta R_{geophysical}\right) \quad (1)$$

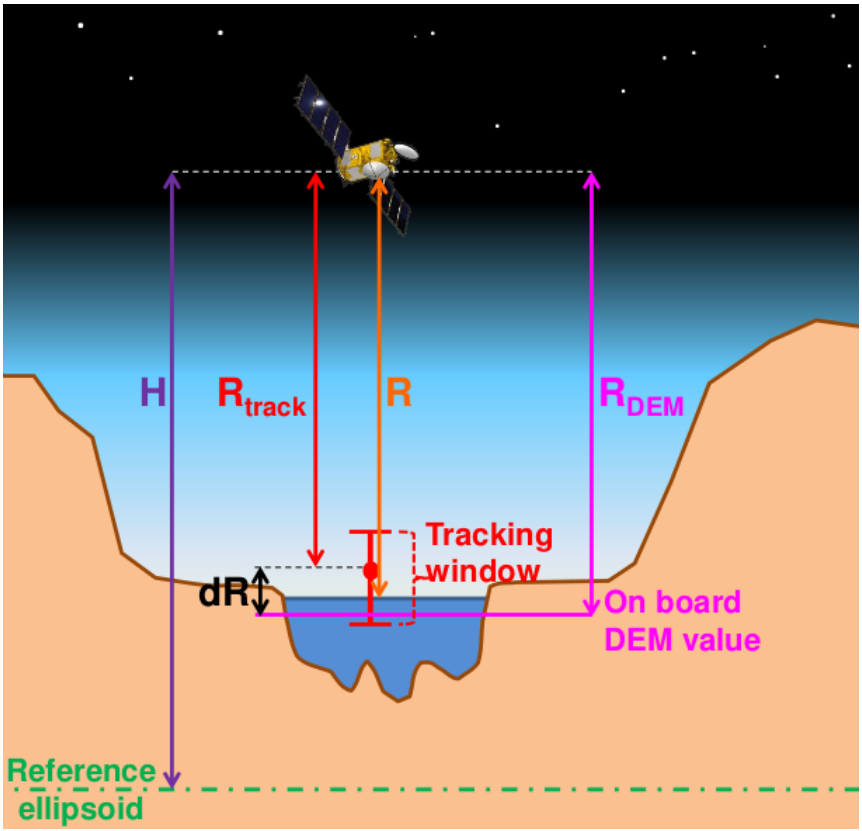

Figure 1. Conceptual view of nadir altimeter measurements and notations used in this study (the copyright of the Jason-3 satellite image used in this sketch belongs to CNES/Mira Production)

This study has processed data from the Jason-2 and Jason-3 altimetry missions. The Jason-2 satellite was launched on 20 June 2008 and was developed by CNES, EUMETSAT (European Organisation for the Exploitation of Meteorological Satellites), NASA, and NOAA (National Oceanic and Atmospheric Administration). Its main payload comprises the Poseidon-3 dual frequency (Ku- and C-bands, 13.575 GHz and 5.3 GHz respectively) radar altimeter (Desjonquères et al., 2010). Jason-2 is on a 10-day repeat cycle orbit at an altitude of 1336 km, and a 66° inclination. Its ground-track spacing is around 315 km at the equator and 220 km over mainland France. Jason-3, developed by the same agencies as Jason-2 plus the European Union (through the Copernicus program), was launched on 17 January 2016 and was put on the same orbit as Jason-2. The two satellites were 80 seconds apart. Jason-3 has a similar payload to

Jason-2, in particular a Poseidon-3 class altimeter (Poseidon-3B). After more than 6 months sharing a common orbit, Jason-2 was put on an "interleaved" orbit on 13 October 2016. This has the same characteristics as its previous orbit, but is shifted in longitude by half the ground-track spacing at the equator.

2.2. Altimeter tracking modes

For technical reasons associated with the pulse compression technique used for emission and owing to the limited signal bandwidth (Chelton et al., 2001), the altimeter records the power returned from the ground over only a limited window of ranges (called "tracking window" on Figure 1). The vertical size of the range window (see Figure 1) for Poseidon-3 class altimeters (i.e. for Jason-2 and Jason-3) is equal to 50 m. As it is orders of magnitude smaller than the altitude of the satellite (around 1336 km), this window needs to enclose the water surface elevation. Otherwise, the altimeter processing unit will not receive any signal backscattered by the river and it will not be possible to derive the actual river elevation. The position of this window (R_{track} on Figure 1) is continuously updated on board to roughly follow the ground topography. This process is called "tracking". It is performed automatically by the Adaptive Tracking Unit (ATU), based on the analysis of waveforms received previously. More information on the ATU system can be found in Chelton et al. (2001) and Desjonquères et al. (2010). This tracking mode is generally referred to as the "autonomous" or "Closed-Loop" (CL) mode. The retracking processing determines the position of the water surface in the waveform (a distance known as epoch). Finally, the range R is estimated using equation (2).

$$R = R_{track} + epoch \quad (2)$$

As nadir altimeters are designed to observe oceans, the ATU is not optimized to follow continental surfaces, where elevations may vary by tens to hundreds of meters over an along-track distance of a few kilometres. This is an issue for steep-sided rivers enclosed in valleys that are a few kilometres wide (i.e. similar to the footprint of the instrument) and more than 50 m (i.e. a distance greater than the tracking window size) lower than the surrounding hills. In this case, the altimeter can remain "locked" on the top of the surrounding hills (or even lose tracking data) and never observe the river below. This problem could even occur with slightly shallower valleys. More detailed explanations and specific examples of this issue can be found, for instance, in Biancamaria et al. (2017).

A new instrument mode, implemented on board Jason-2, SARAL, Jason-3, and Sentinel-3A/B, was designed by CNES and its contractors to solve this specific issue. It consists in setting the tracking window to an *a priori* value close to the river valley elevation, rather than letting the ATU estimate its position based solely on previous waveforms. This solution requires storing on board *a priori* elevation values for targets of interest (e.g. water bodies), as well as their location along the satellite track. Then, the on-board software uses these *a priori* elevations and the altitude of the satellite computed in real time by the DIODE (Doris Immediate Orbit on board Determination) software to force the tracking window to these positions when the satellite overflies them (Desjonquères et al., 2010). To build the on board tables used by the OL tracking mode, an *a priori* list of targets of interest (therefore a water mask) and an elevation associated with each target is required. Accuracies of both target geolocation and associated elevation are crucial to the observation of these water bodies. Therefore, the OL tracking mode has been used on a very small number of cycles on Jason-2 (cycles 3, 5, 7, 34, 209, and 220) and on SARAL (passes 601 to 800 during cycle 1). The elevations used by Jason-2 over France were taken from

the 1 km Altimetry Corrected Elevation global DEM (ACE; Berry et al., 2000) and the water mask from the Generic Mapping Tools (GMT, http://gmt.soest.hawaii.edu/) (Desjonquères, 2009). The *a priori* global DEM used for water body elevations for SARAL was ACE2 (Berry et al., 2010) and the land/water mask was derived from Globcover (http://due.esrin.esa.int/page_globcover.php), supplemented by some water body elevations available on the Hydroweb database.

In OL mode, the leading edge of the waveform (therefore the tracking window, see Figure 1) should ideally be centred on the first third of the tracking window. As this window size is around 50 m for Jason-2 and Jason-3, CNES estimated that the accuracy for water body *a priori* elevations should be around ±10 m.

The OL tracking mode has not been studied extensively. Birkett and Beckley (2010) evaluated both the CL and the OL tracking modes for Jason-2 over 28 lakes and reservoirs. For these targets, they found that CL and OL modes provide similar results when the water body is observed in both modes, but that the CL mode observed more targets than the OL mode. Birkett and Beckley (2010) assumed that ‘‘inadequate resolution and/or data in the DEM” might be the reason for OL mode underachievement in comparison with CL mode. They concluded that the on-board DEM might not be ‘‘optimized for all regions”. Biancamaria et al. (2017) showed that some locations in the steep-sided Garonne River valley (within mainland France) could not be observed by nadir altimeters in CL mode. During the first SARAL cycle, two VS were observed in OL mode. The on-board DEM value for one VS was close to the river valley elevation and therefore the river was observed (which was not the case during subsequent cycles in CL mode). However it was not the case for the second VS. The issue was an incorrect water mask and not a lack of accuracy in the *a priori* DEM used to compute the on-board DEM. For this reason

Biancamaria et al. (2017) concluded that the on-board DEM is highly dependent on both input water mask and the *a priori* DEM used, which should be internally consistent.

The launch of Jason-3 and the need to validate its measurements during 2016 represented a good opportunity to construct a finely tuned on-board DEM over a specific zone, where precise local DEMs are available. The methodology used to achieve this end and the results obtained are presented in the following sections.

3. Methods

3.1. Study domain and a priori/validation data

The study domain chosen to validate Jason-3 measurements over rivers corresponded to mainland France (Figure 2). The four main rivers (ranked by their mean annual discharge at their outlet indicated in brackets) in this study domain are: the Rhône (1700 $m^3.s^{-1}$), the Loire (900 $m^3.s^{-1}$), the Garonne (600 $m^3.s^{-1}$) and the Seine (520 $m^3.s^{-1}$). This region was selected because of the large number of in situ gages operated by regional public agencies, i.e. DREALs (Directions Régionales de l'Environnement, de l'Aménagement et du Logement). These observations are collected by the SCHAPI (Service Central d'Hydrométéorologie et d'Appui à la Prévision des Inondations), which releases them publicly via the online 'Banque Hydro' national database (http://www.hydro.eaufrance.fr) within a period of a few weeks to a few months. Gages used in this study are shown in Figure 2 (green stars). Their records were downloaded from the Banque Hydro database or obtained directly from the operator (DREALs). For all these gages, water elevations measured were referenced to NGF-IGN69, the official vertical reference system for mainland France. Their measurements were available for the period of interest: the tandem phase when Jason-2 and Jason-3 shared the same orbit and ground track. The time series obtained from

these gages have a non-uniform time step, which is dependent on the water elevation stage. Instruments automatically adjust recording time steps to water elevation variations. However, the median time step for all gages is, on average, around 30 minutes.

Figure 2 shows Jason-2/-3 tandem phase orbit tracks (red lines) superimposed on the study domain and their 86 intersections or VS (white and red diamonds) with rivers indicated as wider than 50 m in the IGN (Institut National de l'Information Géographique et Forestière) BD Carthage database (available at www.sandre.eaufrance.fr). The VS with the maximum river width (~300 m) is obtained for the most downstream orbit intersection with the Loire River (near La Ménitré, at -0.280°E and 47.393°N).

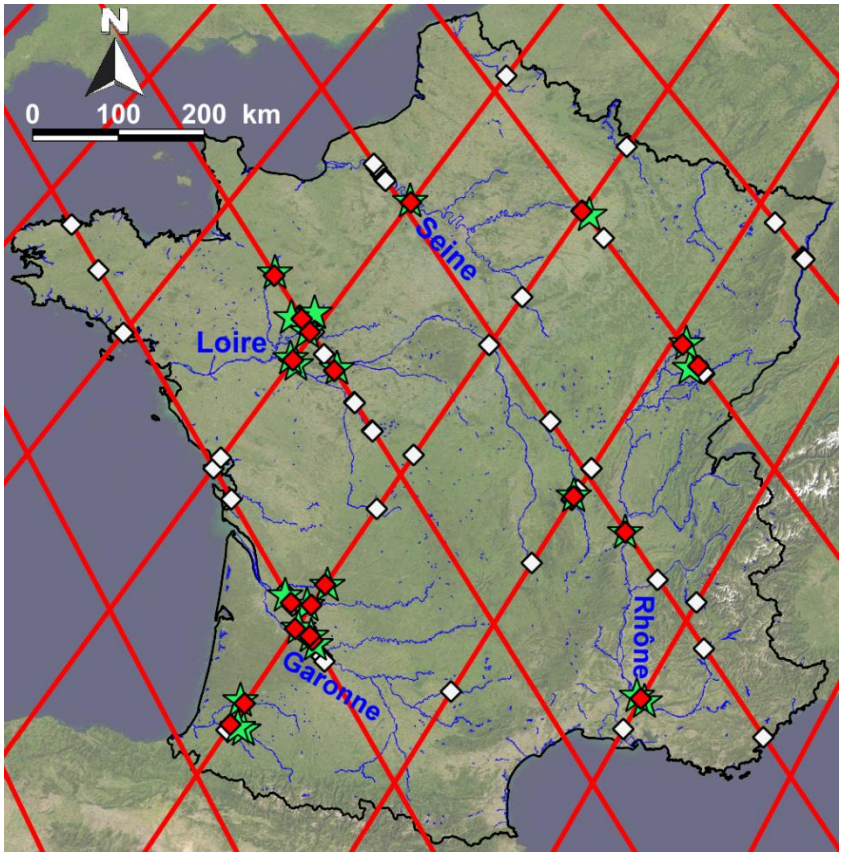

Figure 2. Study domain (Mainland France, delimited by the black line) and the river network (light blue lines) from the IGN BD Carthage database (only rivers wider than 50 m according to this database are shown). Red lines correspond to Jason-2 and Jason-3 tandem phase orbit tracks. White and red diamonds correspond to virtual stations (VS), where Jason-3 on-board DEM values were computed. Red diamonds are virtual stations where Jason-2 and Jason-3 river

elevation time series were compared to in situ gage (green stars) measurements. The background image is derived from the NASA MODIS "Blue Marble Next Generation" image (Stöckli et al., 2005)

3.2. Jason-3 on-board DEM and validation methodology

3.2.1. On-board DEM computation over France

The IGN BD Carthage database with rivers wider than 50 m corresponds to the water mask used in this study. These river reaches were intersected with the Jason-2/-3 orbit obtained from the Aviso+ website (http://www.aviso.altimetry.fr), leading to the creation of 89 VS. Three intersections with the river network and orbit tracks in the most southern part of the Garonne basin (see Figure 2) were not selected. For these locations the on-board DEM has been set by CNES to the altitude of transponders used for calibrating/validating the altimeter.

Next, it was necessary to estimate the DEM values for the 86 selected VS (white and red diamonds on Figure 2). This was achieved using the 25 m resolution DEM from IGN's BD Alti database (http://professionnels.ign.fr/bdalti). The absolute vertical accuracy of this DEM is assessed by IGN at between 2 to 8 m, depending on the local data source used. Elevations are provided as integers and are referenced to the NGF-IGN69 vertical reference system. Rather than simply extracting DEM values at the position of each VS, to take into account the facts that (1) the altimeter ground footprint is a few kilometres wide, (2) the satellite ground track is controlled to within ±1 km around its nominal position (Dumont et al., 2016) and (3) rivers are in the lowest part of the valley, we computed the minimum elevation over a 2 km radius centred on each VS. Different values of this radius have been investigated (1 km to 5 km). A 2 km radius is a good compromise between having sufficient variation to capture the river elevation (when compared to a small number of VS close to a gage) and not being excessively impacted by elevations outside the river valley targeted. As a quality check, the DEM was inspected visually and

290 comparisons made with Google Earth images for the 22 VS where the difference between the
291 minimum elevation computed on this circle and the elevation of the closest Banque Hydro
292 database in situ gage was greater than 10 m. Different cases were observed as follows: the
293 difference was due to an obvious issue with the gage elevation in the Banque Hydro, the closest
294 gage was on a different river to the VS, or the VS was on a reservoir and the gage was not (or the
295 reverse). For each case, the final elevation value was selected manually to take into account the
296 specificity of each case and the local topography in the vicinity of the VS. For all other VS, the
297 minimum elevation on the 2 km circle was selected. This radius might change a little for regions
298 other than France, depending, for example, on the accuracy of the DEM and the water mask. But
299 the methodology should be fairly robust, easily adapted to any other location, and should not be
300 specific to French rivers. Finally, these elevations were sent to CNES, which uploaded them on
301 board Jason-3 on 2 May 2016.

302 3.2.2. Validation of Jason-3 measurements

303 Between 17 February and 2 October 2016, Jason-2 (cycles 281 to 303) and Jason-3 (cycles 1 to
304 23) flew on the same orbit, 80 seconds apart. Therefore, they observed the same locations almost
305 simultaneously, which allowed the direct comparison of measurements from both satellites.
306 Jason-2 was in CL tracking mode throughout the study period, whereas thirteen Jason-3 cycles
307 were in OL tracking mode, for the most part after May 2016 (see Table 1 for cycle numbers and
308 start dates). Therefore, it is possible to evaluate the benefits of the OL tracking mode for small to
309 medium-sized steep-sided rivers by comparing Jason-3 cycles in OL mode to Jason-2 data and in
310 situ measurements.

Table 1. Number and start times of Jason-3 cycles in OL tracking mode, during the shared orbit period with Jason-2

Jason-3 cycles in OL tracking mode	Cycle start time

9	06 May 2016
11	26 May 2016
12	05 June 2016
13	15 June 2016
14	25 June 2016
15	05 July 2016
16	15 July 2016
17	25 July 2016
18	04 August 2016
19	13 August 2016
21	02 September 2016
22	12 September 2016
23	22 September 2016

311

312 To validate Jason-3 measurements (section 4), an initial qualitative test was performed to
313 compare Jason-2 and Jason-3 measurements over the 86 VS. For each VS, the absolute
314 difference (noted dR on Figure 1) between R_{track} (the tracked distance between the satellite and
315 the tracking window, see Figure 1 and section 2.2) and R_{DEM} (the distance between the satellite
316 and the position of the surface given by the DEM, see Figure 1) was computed. dR allows to
317 quantitatively estimate how the position of the tracking window in CL mode is far from the on
318 board DEM value (which should be close to the river elevation). Figure 1, illustrates a case when
319 Jason-3 in CL mode successfully observes the river. In this case, dR is smaller than the size of
320 the tracking window. Therefore, dR should provide useful information to assess if a SV in CL
321 mode observe the river (dR much smaller than 50 m) or the surrounding topography (dR higher
322 than 50 m). That's why, in section 4, its temporal mean value for Jason-3 cycles in CL mode is
323 analysed. Similar averages were computed for corresponding Jason-2 data during the same

cycles. It allowed us to estimate, on average, how the tracked elevation differs between Jason-2 and Jason-3, when their altimeters are both in CL mode and when Jason-3 is in OL mode and Jason-2 is in CL mode. In addition, the backscatter coefficient, which takes a high value in the event that water contributes to the power recorded by the altimeter (e.g. Frappart et al., 2015c), was analysed.

For quantitative validation, all VS close to a "Banque Hydro" in situ gage were selected. For these VS, Jason-2 and Jason-3 measurements were processed to extract elevation time series (see section 2.1), without using any *a priori* information from the gage time series. Jason-3 time series were computed using all available measurements, without differentiating between cycles in CL mode and in OL mode. For both Jason-2 and Jason-3, some cycles had valid measurements of river elevations for many VS, whereas other cycles measured the elevations of the surrounding topography. Measurements from the latter cycles were easily excluded, as they were much higher than those of valid cycles. For this reason, some VS time series present observation gaps.

A thorough inspection led to the selection of 24 in situ gages (Figure 2, green stars) which were compared to 21 VS (Figure 2, red diamonds). The number of VS selected was different to the number of gages selected, as some VS had two in situ gages sited nearby (one upstream and one downstream), or conversely, some gages were sited close to two VS. The selection criteria were that (1) the distance between gages and VS should be a few kilometres, (2) they should be located on the same river with no large intervening tributaries, and (3) the in situ gage time series should be available from the Banque Hydro or directly from regional DREAL agencies (see section 3.1). More information (WGS84 longitude/latitude coordinates, river width, and the intervening distance) for each pair of gage and VS compared is presented in the supplementary material.

To carry out this quantitative assessment for validation purposes, Jason-2 and Jason-3 time series were both compared to the in situ gage time series, using the same statistical tests as Biancamaria et al. (2017): correlation coefficient, mean bias, and Root Mean Square Error (RMSE) between the two time series for absolute water elevations referenced to NGF-IGN69. In situ and altimetry water elevation anomalies were also computed, by removing their respective temporal mean (calculated for the same common dates). The RMSE and the Nash-Sutcliffe (NS) coefficient (Nash and Sutcliffe, 1970) were computed for anomalies. The NS coefficient (which varies between $-\infty$ and 1) was used in this study for its ability to assess the accuracy of the match between two time series, both in time and amplitude. It is more informative than the correlation coefficient, which only provides information about the linear relationship between two time series, without taking into account amplitude agreement (Moriasi et al., 2007). The NS coefficient for absolute elevation is not provided, as a bias is expected between altimetry measurements and the gage time series, caused at least partly by the slope of the river between the VS and the gage.

The Jason-2 and Jason-3 data used in this study were taken from the Geophysical Data Records (GDR), version D, provided by the CNES/NASA processing centres and formatted by the Centre de Topographie de l'Océan et de l'Hydrosphère (CTOH, http://ctoh.legos.obs-mip.fr) in a consistent NetCDF format with geophysical corrections coherent with previous altimetry missions. The retracking algorithm used in this study is Ice-1/ICE (Wingham et al., 1986), as recommended by Frappart et al. (2006) for continental surfaces. Water elevation time series were computed using Multi-mission Altimetry Processing Software (MAPS) that allows a refined selection of valid altimetry data to build VS (Frappart et al., 2015b). MAPS is a graphical user interface that allows the loading of altimetry data formatted by CTOH that are located within the

boundaries of a VS polygon, the computation of water elevations using Eq. 1 and the manual selection/removal of some measurements. These water elevations provided by MAPS correspond to ellipsoid heights. They have then been referenced to NGF-IGN69, for comparison to in situ water elevation time series.

4. Results

4.1. Jason-3 statistics over the study domain

Figure 3 shows maps of Jason-2 and Jason-3 absolute difference dR (see section 3.2.2 and Figure 1), averaged over Jason-3 CL mode cycles (Figure 3.a and 3.c) and those where Jason-3 is in OL mode (Figure 3.b and 3.d). As the size of the Jason-2 and Jason-3 tracking window is around 50 m, wherever and whenever this difference is greater than 50 m (Figure 3, red diamonds), it can be assumed that the altimeter is locked on the surrounding hills. This figure clearly shows that Jason-2 behaved in a similar manner before (Figure 3.a) and after (Figure 3.b) May 2016. It also shows that Jason-3 exhibited similar behaviour to that of Jason-2 when it was in CL tracking mode (Figure 3.c), with a slight tendency to have a few more VS locked on the surrounding hills (especially in the downstream part of the Garonne River).

Table 2 summarizes these results by showing some basic information for the 86 VS. Jason-2 behaves consistently over the whole time period. Therefore, the differences between the Jason-3 measurements in CL and OL modes can only be explained by the differences in tracking mode. For Jason-2, 25 VS (29% of all VS) are always locked on the top of the topography (first line in Table 2). This number increases to 38 VS (44%) for Jason-3 in CL mode. Around half of the VS had some cycles affected by this behaviour, as 34 (40 %) VS (Jason-2) and 49 (57 %) VS (Jason-3 in CL mode) have an average dR of over 50 m. Table 2 also indicates the mean and the

maximum values of the backscatter coefficient σ_0 (in dB) averaged over all VS. The average value of σ_0 over all VS is equal to 29 dB and 25 dB for Jason-2 and Jason-3 in CL mode, respectively. σ_0 tends to be lower over land than over water (smoother and more reflective surface than land, e.g. Frappart et al., 2015c). Therefore, its lower value for Jason-3 measurements in CL mode confirms its tendency to be locked on the surrounding topography more often than Jason-2. Nevertheless the σ_0 for both altimeters remain close. However, the average σ_0 for Jason-3 in OL mode increased to 40 dB, confirming that Jason-3 in OL mode observed more rivers than Jason-2. However, it is not sufficient to show that the signal backscattered by the river is measured by the altimeter. There remains the task of checking that these measurements can be converted to useful water elevation time series. For this reason, the next section compares the Jason-2 and Jason-3 time series to in situ water elevation time series.

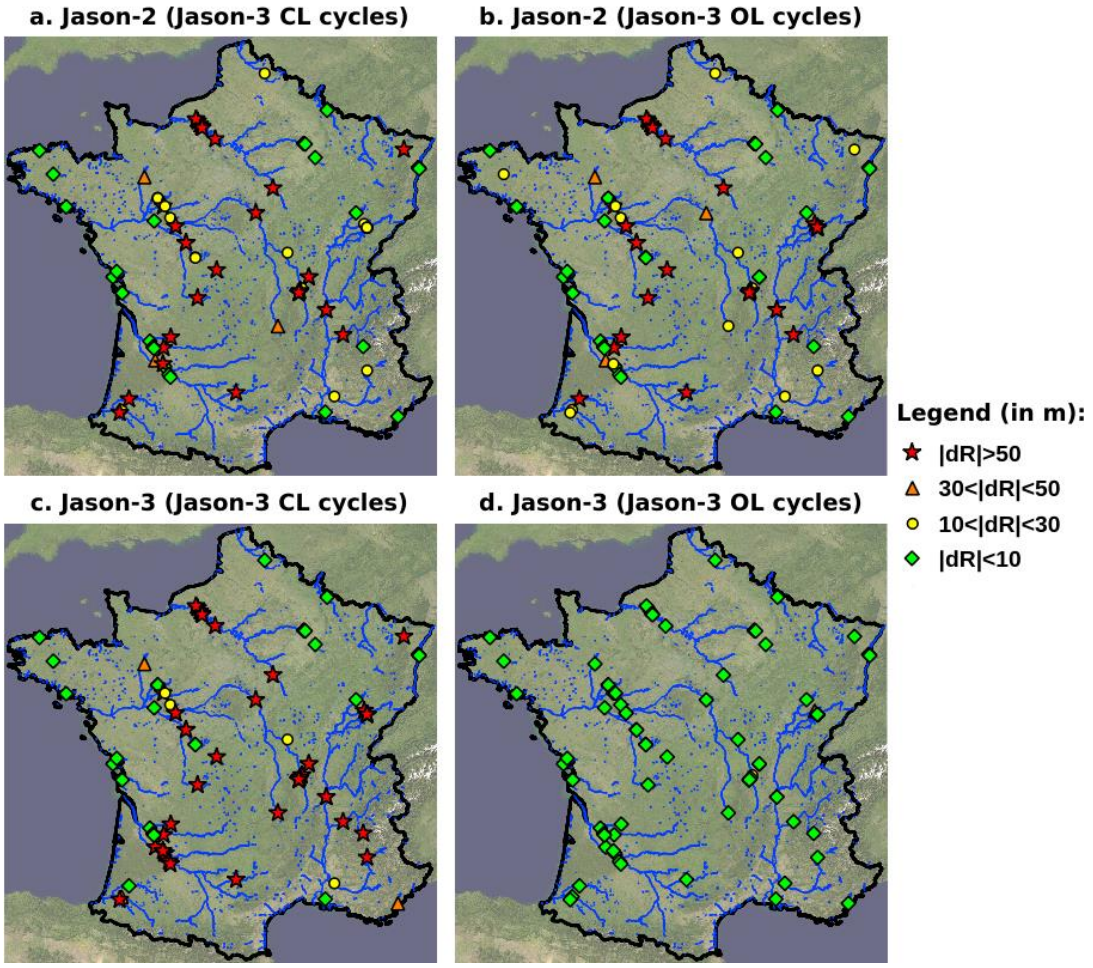

404

Figure 3. Mean absolute difference (dR) between R_{track} and R_{DEM} (see Figure 1) for Jason-2 (a. and b.) and Jason-3 (c. and d.) for cycles when Jason-3 is in closed-loop mode (approximately between February and May, 2016; a. and c.) and when Jason-3 is in open-loop mode (approximately between May and September, 2016, see Table 1 for the list of cycles; b. and d.)

405

Table 2. Statistics computed using the 86 VS shown on Figure 2 (red and white diamonds) indicating the number of VS for which the min, max, and mean difference between the altimeter tracked height and on-board DEM values (dR) is greater than the size of the tracking window (50 m), values of the mean and max dR (in m) over all VS and the mean and max backscatter coefficient σ_0 (in dB) over all VS

	Jason-2 (J-3 CL cycles)	Jason-3 (CL cycles)	Jason-2 (J-3 OL cycles)	Jason-3 (OL cycles)
Nb VS with min(dR) > 50m	25	38	24	0
Nb VS with mean(dR) > 50m	34	49	35	0
Nb VS with	50	55	50	0

max(dR) > 50m				
Mean(dR) (in m)	50	82	51	-2
Max(dR) (in m)	311	720	299	31
Mean(σ_0) (in dB)	29	25	30	40
Max(σ_0) (in dB)	54	56	53	54

406

407 4.2. Validation of Jason-3 data for the selected gages

408 This section focuses on the 21 VS (Figure 2, red diamonds) that are close to in situ gages (Figure
409 2, green stars) which were selected for a quantitative assessment of Jason-2 and Jason-3 errors
410 (see section 3.2.2).

411 Table 3 and Table 4 show the comparative statistics for in situ, and Jason-2 and Jason-3 satellite
412 time series, respectively, for all VS/gage pairs. Data shown in these two tables suggest that
413 altimeters are capable of accurately monitoring some small rivers, such as the JA-002 VS on the
414 Marne River, which is 40 m wide. On this river both Jason-2 and Jason-3 display an RMSE of
415 0.20 m for water elevation anomalies, whereas the amplitude of the in situ time series at the
416 satellite observation times is much larger (2.72 m). However, this instance is very favourable for
417 altimetry, as the topography is quite flat, with little surrounding vegetation. For Jason-2,
418 correlation coefficients greater than 0.9 are associated mainly with rivers wider than 130 m,
419 whilst for Jason-3, correlation coefficients greater than 0.9 are mainly associated with rivers
420 wider than 100 m. The Jason-2 RMSE for elevation anomalies for these rivers ranged from 0.20
421 to 0.63 m, whereas the Jason-3 RMSE was between 0.11 and 0.28 m. Eight Jason-2 VS (38% of
422 VS selected) were significantly impacted by the surrounding topography, with fewer than 5
423 cycles (out of 23) observing the river valley or with a bias compared to in situ measurements
424 around 50 m or more. All of these VS were observed correctly by Jason-3 only when operating in

OL mode (except for JA3-014 for which 7 cycles in CL mode observed the river valley) with a small bias for absolute elevation compatible with what might be expected from the river slope (a couple of metres over a distance of a few kilometres). The same statistics as those shown in Table 3 and 4, but computed only for Jason-3 CL mode cycles and Jason-3 OL mode cycles for both Jason-2 and Jason-3, are presented in the supplementary material associated with this article. They show that the accuracy of Jason-3 measurements is fairly similar for those VS that work well in both CL and OL modes. This result indicates that the OL tracking mode is operating as expected and allows the observation of steep-sided rivers that previously were practically never observed, resolving the issue described in Biancamaria et al. (2017). It should also be noted that Jason-3 observed the river valley for all VS during the 13 OL mode cycles. In Table 4, for VS with only 13 cycles in their time series, these cycles correspond solely to OL mode cycles (there are no observations for CL cycles). This is shown clearly in the tables presented in the supplementary material. There are three Jason-3 VS (JA3-075, JA3-017, and JA3-010) that are always locked on the surrounding topography in CL mode (0 cycle used in Table 4 in the supplementary material), whereas the corresponding Jason-2 VS provide some measurements of the river elevation (i.e. two or more cycles could be used, their bias with in situ measurements is below 50 m, and their correlation coefficient with in situ measurements is above 0.50).. However, it should be noted that, for JA-075 and JA-017 VS, unlike JA-010 VS, even for Jason-3 OL mode cycles or Jason-2 cycles with valid measurements, the RMSEs for water elevation anomalies are still large, because of the small river widths (see supplementary material for these RMSEs). For other Jason-3 VS with 0 cycle used in CL mode, Jason-2 does not provide useful measurements of the river elevation (see supplementary material). For some other VS, the Jason-3 time series had fewer observation dates than the corresponding Jason-2 time series, owing to

there being more Jason-3 cycles in CL tracking mode locked on the surrounding topography (see table in supplementary material). This is consistent with the results obtained by the qualitative assessment (section 4.1).

Table 3. Correlation coefficient, mean bias, RMSE (m), RMSE for anomalies (m), Nash-Sutcliffe (NS) coefficient for anomalies between Jason-2 and in situ time series. River width at the VS, amplitude (Ampl.) of the in situ time series for dates in common with Jason-2, and the number of these common dates are also provided. Rows shaded red correspond to VS/gage pairs for which the mean bias is around 50 m or more and/or the correlation coefficient is below 0.5 and the NS coefficient for anomalies is negative. Rows shaded orange correspond to VS for which half or more cycles are locked on the surrounding topography (11 or less cycles used)

Jason-2 VS ID	VS Riv. Width (m)	Gage ID	Corr.	Bias	RMSE (m)	RMSE anom (m)	NS anom	Ampl. (m)	Nb cycles used
JA2-074	35	M1511610	0.62	3.33	3.35	0.30	0.26	1.46	23
JA2-075	35	M3230930	0.47	26.07	26.07	0.25	-0.39	0.65	17
JA2-002	40	H5201010	0.97	-2.23	2.24	0.2	0.95	2.72	23
JA2-017	40	U1074020	0.43	12.55	12.57	0.64	0.15	2.64	12
JA2-011	45	P7121510	-	0.25	0.25	-	-	-	1
JA2-014	45	Q1420010	0.88	3.67	3.7	0.44	0.63	1.85	4
JA2-077	45	X3310010	-0.16	-11.39	11.51	1.63	$-3.5x10^4$	0.05	23
JA2-077	45	X3500010	-0.25	16.42	16.51	1.67	-76.79	0.83	20
JA2-020	60	U0610010	0.87	1.44	1.49	0.39	0.75	3.14	22
JA2-071	60	M0520610	0.62	-5.59	5.59	0.15	0.30	0.59	20
JA2-071	60	M0630610	0.62	5.56	5.57	0.18	0.38	0.71	17
JA2-042	70	K0910010	0.56	1.04	1.16	0.5	-2.05	0.78	5
JA2-012	80	Q5421020	0.8	-34.32	34.32	0.32	0.53	1.56	19
JA2-012	80	Q5501010	0.76	13.73	13.74	0.36	0.30	1.35	19
JA2-094	90	V3130021	0.4	127.92	127.93	2.02	-5.43	1.97	11
JA2-009	110	P5550010	-	3.96	3.96	-	-	-	1
JA2-093	120	V3130021	0.1	126.9	126.96	3.74	-23.98	1.97	13
JA2-010	130	O9190010	0.97	-0.15	0.43	0.4	0.93	4.36	8
JA2-030	155	O9090010	0.91	3.58	3.64	0.63	0.75	4.37	23
JA2-030	155	O9000010	0.91	-3.01	3.08	0.63	0.78	4.53	23
JA2-080	165	H8100021	0.55	82.39	82.4	0.14	0.31	0.66	12
JA2-032	200	O9090010	0.95	0.96	1.03	0.37	0.89	3.56	10
JA2-036	245	P5770010	0.74	3.89	3.98	0.81	-51.61	0.38	20
JA2-064	250	K6830020	0.47	49.18	49.28	3.19	-8.54	3.28	23
JA2-082	300	L8700020	0.99	-0.09	0.37	0.36	0.93	5.5	23
JA2-082	300	L8700030	0.99	1.74	1.75	0.19	0.97	4.73	23

Table 4. Correlation coefficient, mean bias, RMSE (m), RMSE for anomalies (m), Nash-Sutcliffe (NS) coefficient for anomalies between Jason-3 and in situ time series. River width at the VS,

amplitude (Ampl.) of the in situ time series for dates in common with Jason-3, and the number of these common dates are also provided. Rows shaded red correspond to VS/gage pairs for which the correlation coefficient is below 0.5 and the NS coefficient for anomalies is negative

Jason-3 VS ID	VS Riv. Width (m)	Gage ID	Corr.	Bias	RMSE (m)	RMSE anom (m)	NS anom	Ampl. (m)	Nb cycles used
JA3-074	35	M1511610	0.71	2.92	2.94	0.31	0.24	1.46	22
JA3-075	35	M3230930	-0.27	-1.45	1.68	0.85	-26.69	0.74	13
JA3-002	40	H5201010	0.97	-2.62	2.63	0.2	0.95	2.72	23
JA3-017	40	U1074020	0.13	11.67	11.7	0.8	-0.49	2.48	13
JA3-011	45	P7121510	0.86	-0.71	0.88	0.52	-15.34	0.46	13
JA3-014	45	Q1420010	0.84	3.49	3.5	0.23	0.67	1.52	20
JA3-077	45	X3310010	0.35	-12.04	12.13	1.47	$-2.6x10^4$	0.05	21
JA3-077	45	X3500010	0.25	15.77	15.84	1.45	-53.61	0.82	18
JA3-020	60	U0610010	0.84	1.11	1.18	0.42	0.7	3.14	22
JA3-071	60	M0520610	0.55	-5.91	5.92	0.19	-0.10	0.59	21
JA3-071	60	M0630610	0.51	5.25	5.25	0.21	0.11	0.71	18
JA3-042	70	K0910010	0.94	0.1	0.23	0.21	0.85	1.78	13
JA3-012	80	Q5421020	0.64	-34.83	34.84	0.45	0.2	1.55	18
JA3-012	80	Q5501010	0.65	13.23	13.24	0.42	0.03	1.35	18
JA3-094	90	V3130021	1	0.32	0.33	0.11	0.99	2.6	12
JA3-009	110	P5550010	0.99	2.42	2.43	0.14	0.97	2.94	13
JA3-093	120	V3130021	1	0.51	0.56	0.24	0.94	2.6	13
JA3-010	130	O9190010	0.99	-0.71	0.73	0.16	0.97	2.84	13
JA3-030	155	O9090010	0.95	2.44	2.46	0.28	0.9	2.52	16
JA3-030	155	O9000010	0.96	-4.13	4.13	0.27	0.92	2.6	16
JA3-080	165	H8100021	0.95	0.19	0.34	0.28	0.64	1.76	13
JA3-032	200	O9090010	0.99	0.4	0.42	0.14	0.98	2.52	16
JA3-036	245	P5770010	0.7	3.81	4.01	1.26	-127.05	0.38	21
JA3-064	250	K6830020	0.98	1.54	1.56	0.21	0.96	3.28	13
JA3-082	300	L8700020	0.99	-0.53	0.60	0.28	0.96	5.5	22
JA3-082	300	L8700030	0.99	1.29	1.31	0.20	0.97	4.73	22

Figures 4, 5, and 6 show the comparison of elevation time series derived from Jason-2 and Jason-3 against in situ data for three pairs of VS/gage: JA-082/L8700020, JA-030/O9000010, and JA-064/K6830020, respectively. Blue lines and dots correspond to gage time series, whereas red lines and dots correspond to nadir altimetry measurements. For the altimetry time series, the grey vertical bar for each observation time corresponds to the mean absolute deviations of all selected altimetry measurements for that time within the VS boundaries computed by MAPS software (see section 2.1 and for more details Frappart et al., 2015b and Biancamaria et al., 2017).

In the case shown in Figure 4, Jason-3 cycles perform well in both CL and OL tracking modes, similarly to Jason-2. It shows that the OL mode, when the on-board DEM is accurate, performs as well as the CL mode with valid cycles. Both modes perform well probably because there is an elevation difference of less than 50 m between the surrounding hills and the river valley. The high mean absolute deviation for one Jason-3 cycle (early April 2016) shown in Figures 4.b and 4.d is due to an outlier in the selected points within the VS, which may correspond to a measurement of the surrounding topography. In the case shown in Figure 5 all Jason-2 cycles (i.e. in CL tracking mode) observe the river, whereas only 3 (out of 10) Jason-3 cycles in CL (and all cycles in OL) observe the river. Finally, Figure 6 illustrates a Jason-2 VS that never observes the river and remains locked on the surrounding hills, whereas only Jason-3 cycles in OL mode are able to measure the river elevation. All these figures, and in particular their bottom panels show that a Jason-2/-3 sampling period of 10 days is coarse for this type of river. Combining measurements from multiple altimetry missions might be beneficial here. The study time period (mid-February to late September 2016) covered a period of high flows (February/March), a flooding event on the Loire River lasting several days (in early June 2016) and a low flow period (July/September). The altimeter time series allowed sampling of the seasonal cycle (transition from high to low flow periods), but missed local maxima, especially the flood peak on the Loire at VS JA3-064. As previously stated by Biancamaria et al. (2017), Jason-2/-3 time sampling allows the study of the seasonal cycles of small to medium-sized rivers, but will miss high frequency dynamics (periods of hours to a few days). Having measurements of this kind will not assist flood forecasting for the type of rivers presented in this study, but they are important for studying the seasonal cycle, the annual, interannual, and even decadal dynamics of small and medium-sized rivers, especially in areas where no gaging

network is present or maintained. The OL tracking mode will help to obtain more observations from around the world for these types of river.

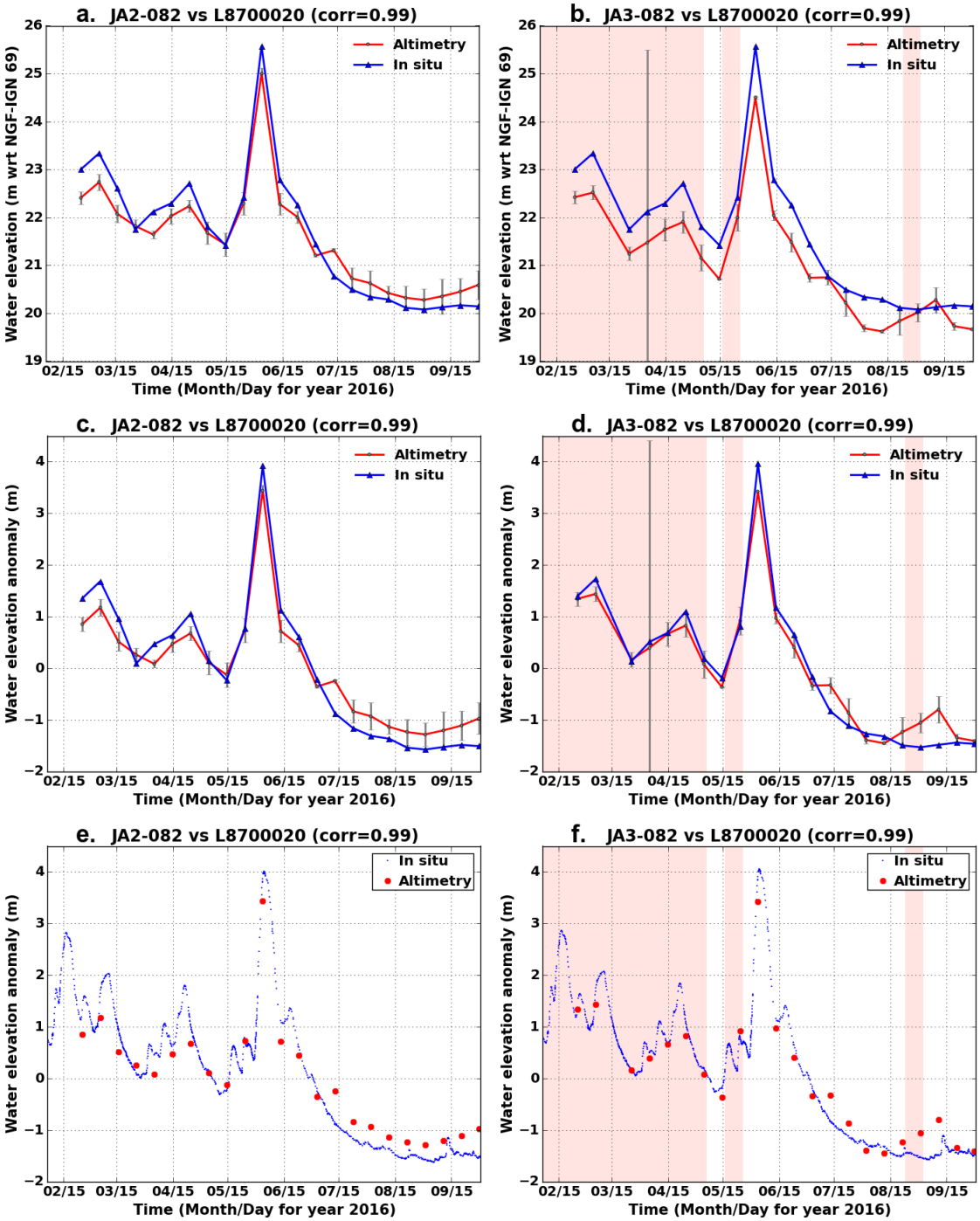

Figure 4. Jason-2 (left panels; a., c. and e.) and Jason-3 (right panels; b., d. and f.) water elevation time series (red lines and red dots) on the Loire River at La Menitré (JA-082) compared to in situ time series (blue lines and blue dots) at Gennes. Top panels (a. and b.) correspond to absolute elevations with reference to (wrt) NGF-IGN69 at satellite observation

times. Middle panels (c. and d.) correspond to elevation anomalies at satellite observation times. Bottom panels (e. and f.) correspond to times series with all available times for both satellite and in situ time series. Pale rose zones on panels b., d., and f. correspond to time periods when Jason-3 altimeter was in CL tracking mode

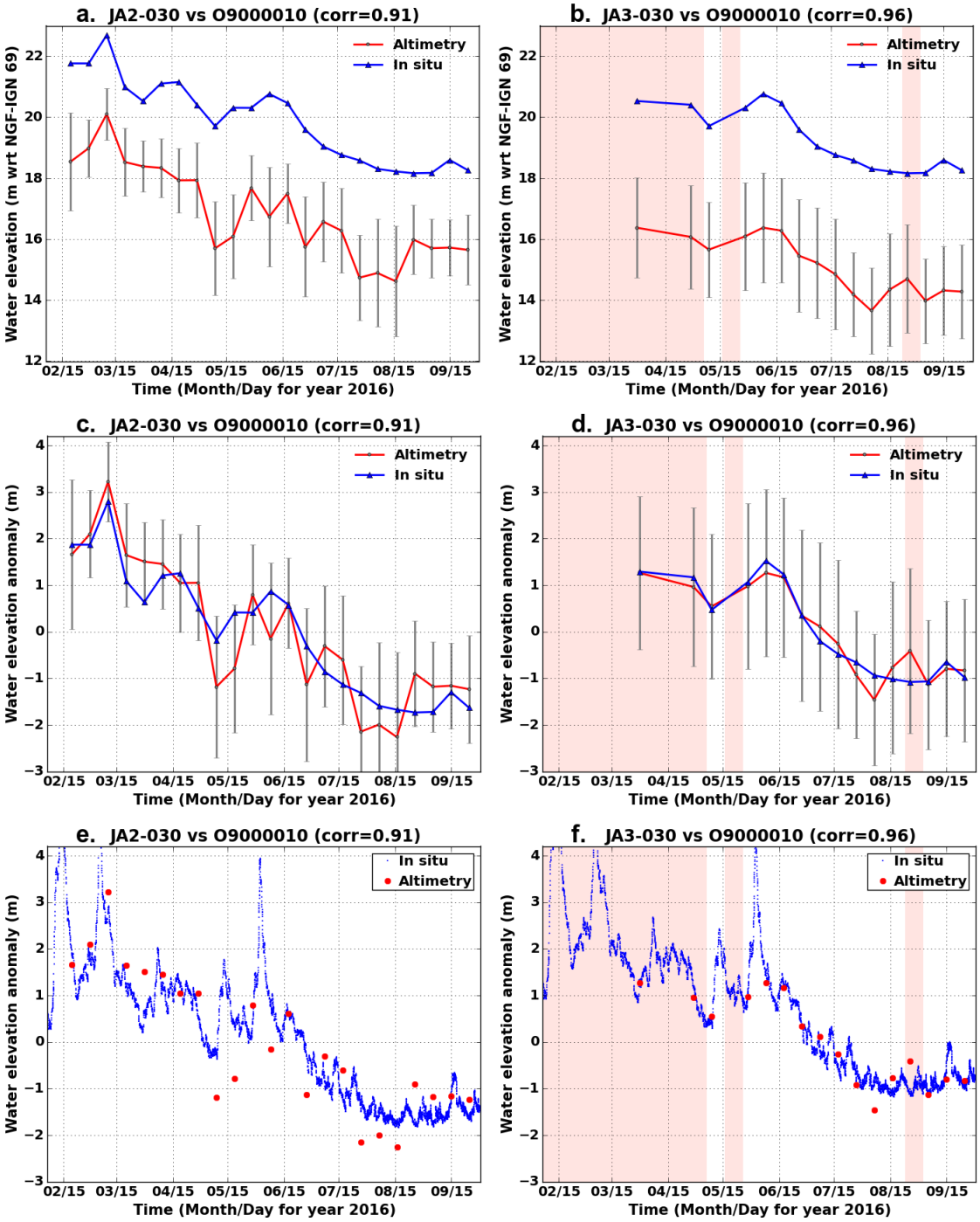

Figure 5. Jason-2 (left panels; a., c. and e.) and Jason-3 (right panels; b., d. and f.) water elevation time series (red lines and red dots) on the Garonne River at Caumont-sur-Garonne (JA-030) compared to in situ time series (blue lines and blue dots) at Tonneins. Panels are

similar to those in Figure 4. Pale rose zones on panels b., d., and f. correspond to time periods when Jason-3 altimeter was in CL tracking mode

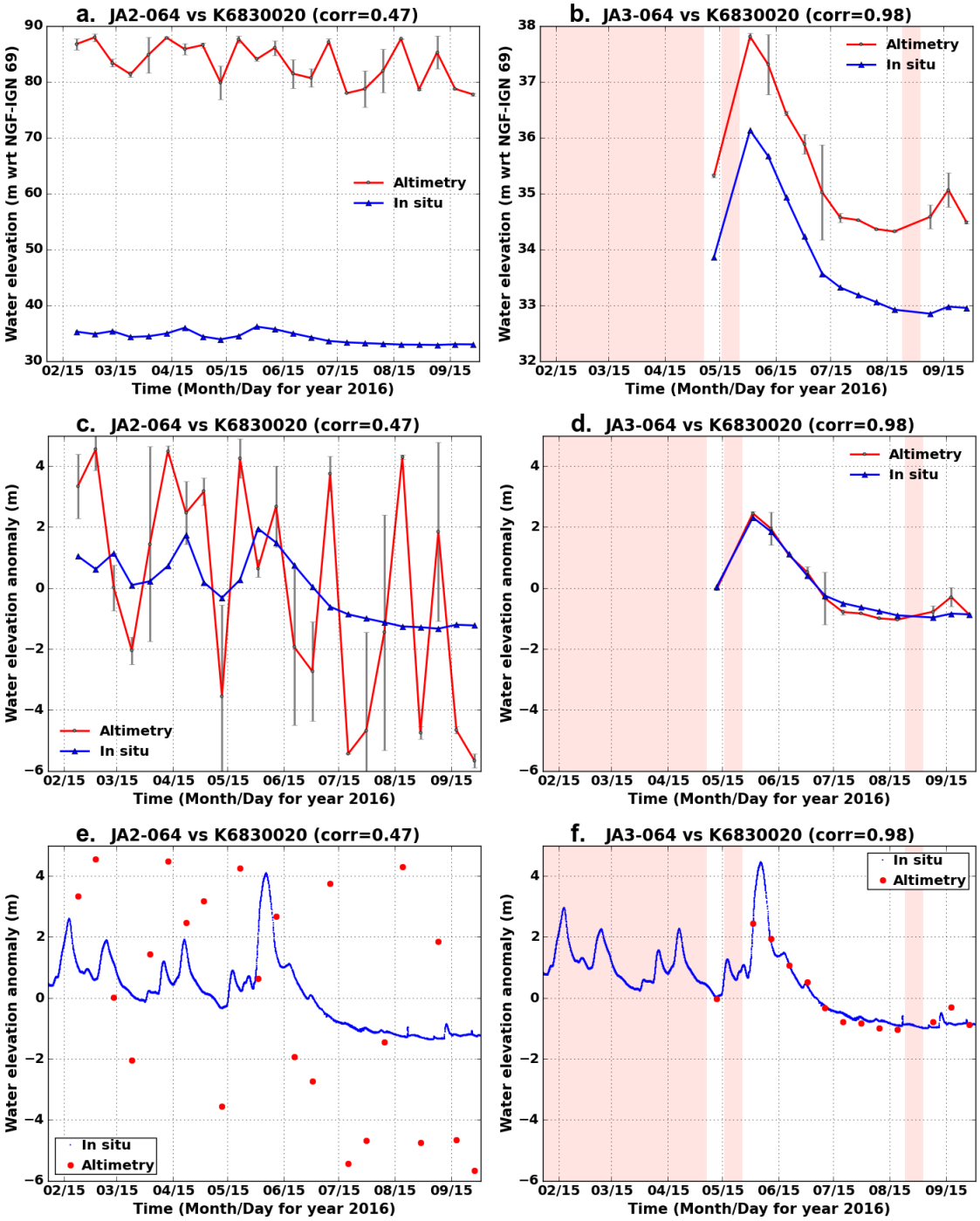

Figure 6. Jason-2 (left panels; a., c. and e.) and Jason-3 (right panels; b., d. and f.) water elevation time series (red lines and red dots) on the Loire River at Saint-Michel-sur-Loire (JA-064) compared to in situ time series (blue lines and blue dots) at Langeais. Panels are similar to those in Figure 4. As Jason-2 is locked on the surrounding topography, panels c. and e. are not

relevant, but are kept for consistency with Figure 4 and Figure 5. Pale rose zones on panels b., d., and f. correspond to time periods when Jason-3 altimeter was in CL tracking mode

4.3. Discussion on the difference between Jason-2 and Jason-3 performance in CL mode

Results from both qualitative (section 4.1) and quantitative (section 4.2) Jason-3 validation assessments showed that Jason-3 in CL tracking mode was more frequently locked on the surrounding topography than Jason-2. Jason-3 and Jason-2 altimeters use the same CL tracking algorithm, called the median tracker. The aim of the median tracker is to "track" as much backscattered energy from the ground as possible, in the hope that the tracked ground corresponds to water bodies. This is a statistical approach, which almost always works, but which does not discriminate between surface types. In other words, in CL tracking mode we cannot give preference to water bodies over other ground targets. The fact that Jason-2 tracks more hydrological targets than Jason-3 in CL mode may appear to be counterintuitive. Although Jason-2 and Jason-3 share a common algorithm, the hardware is not exactly the same. Algorithm parameters values must be adapted to each instrument. They are defined during altimeter ground tuning and testing. These are critical values and are generally not updated in flight unless strictly necessary. Owing to some unexpected in-flight behaviour of Jason-2 ("ghost echoes") the post-launch modification of the original tuning of the altimeter was unavoidable. A side-effect of this procedure was a slight degradation of radar sensitivity in CL tracking mode. When the altimeter operates in CL mode, it first searches for a backscattered radar signal. For this purpose, it scans from higher to lower altitudes. Then when the energy received by the altimeter is sufficiently strong with respect to its sensitivity, it stops scanning altitudes and locks its tracking loop to the current target altitude.

In the case of areas with relief, generally the higher the altitude, the weaker the backscattered signal. As the sensitivity of the Jason-2 altimeter has been degraded, the result is that, in principle, for such regions, it will lock its tracker at a lower altitude than the Jason-3 altimeter. As rivers are particularly located in valleys, Jason-2 will have a better chance of tracking a hydrological target than Jason-3.

The drawback of the median and more generally the CL tracker is the lack of control and of target prioritization. For this reason, the OL tracking mode was designed to overcome this issue. It has the capability to designate a target and therefore to give highest priority to water bodies. Prior to the Jason-3 launch, it was not anticipated that Jason-2 altimeter tuning was improving water elevation observation over continents. As this modification was not applied to Jason-3 (or to any other past, present or planned altimeter), it should be expected that Jason-3 in CL tracking mode will be locked over surrounding topography for steep-sided rivers more frequently than Jason-2, as shown in this study. However, the yield of Jason-3 in OL tracking mode will be dramatically better than that of Jason-2 if the behaviour observed over mainland France, can be obtained for all global locations.

5. Conclusions and Perspectives

The 6 month period during which the recently launched Jason-3 altimetry mission shared the same orbit as Jason-2 was the perfect time to validate the Jason-3 Closed-Loop (CL) tracking mode and to assess the benefit of the Jason-3 Open-Loop (OL) tracking mode. A high-quality DEM and water mask available from the IGN were used to compute the on-board DEM for the OL mode over mainland France which was loaded onto Jason-3 on 2 May 2016 (the first Jason-3

cycles being in CL tracking mode). Accurate water elevations from in situ gages were used to validate both Jason-2 and Jason-3 measurements for river widths between 35 and 300 m.

This study has shown that altimeters such as Jason-2 and Jason-3 are able to accurately measure rivers with a width of 100 m or greater with an RMSE for elevation anomalies of around 0.20 to 0.30 m. The 10 day sampling period is adapted for observing the seasonal cycle, but misses some local maxima. Smaller rivers could also be observed, but with a higher RMSE and time sampling could be more critical for this type of river.

This study demonstrates that Jason-2 and Jason-3 in CL mode provide similar results, although Jason-3 has a tendency to remain locked on the surrounding topography more frequently than Jason-2. This issue is due to a Jason-2 altimeter post-launch tuning, which solved a problem but led to a slight degradation in radar sensitivity. It was not anticipated that this modification would improve observations over continents. As the problem had been resolved on the Jason-3 altimeter, this modification was not applied to the Jason-3 CL tracking mode. Of the Jason-2 VS, 38% measured the top of the surrounding hills almost all of the time. On the contrary, water elevation measurements were always measured at the corresponding Jason-3 VS in OL mode. Even for Jason-2 VS that were only partially affected by this issue (a small number of cycles locked on the surrounding topography), Jason-3 was able to observe the river in OL mode for all cycles, increasing the number of observation times. This shows the significant advantages provided by the OL tracking mode for steep-sided rivers that were unobserved or only partially observed by previous altimetry missions, thus potentially significantly increasing the number of river reaches that could be monitored worldwide by satellite radar altimeters. Even much wider rivers could benefit from the OL tracking mode if they are located in a narrow river valley (a few kilometres across), or are very close to surrounding hills that are higher than the river elevation

by 50 m or more. Jason-3 has greater flexibility than previous missions (i.e. Jason-2 and SARAL) had in OL mode, because small portions (a few kilometres) of the track can be in OL tracking mode (for locations where the water mask and the *a priori* DEM are coherent and sufficiently accurate), while the rest of the track remains in the classical CL tracking mode. Demonstrating the potential of the OL tracking mode is important in the early stages of the Jason-3 mission and also in the context of recently launched (Sentinel-3A), or future altimetry missions (Sentinel-3B planned for launch in early 2018, Sentinel-3C/D whose launch dates are currently unknown, as they will ensure continuity of observation after Sentinel-3A/B, Jason-CS/Sentinel-6 in 2020, SWOT in 2021, and follow-ons), that operate or will operate using this tracking mode. The use of the OL tracking mode will substantially increase the number of river basins that can be monitored using satellite radar altimetry.

The OL mode over mainland France successfully provided observations of river stages, because an accurate on-board DEM could be computed, based on accurate local database. Unfortunately, such a database is not available globally and other sources will have to be used for the rest of the world. For some locations where the global DEMs (GDEM) are sufficiently accurate, these could be used to compute the on-board DEM for OL mode. This could be the case for GDEMs such as the latest version of the Shuttle Radar Topography Mission GDEM released in September 2014 (see https://www2.jpl.nasa.gov/srtm/), the ASTER GDEM (Tachikawa et al., 2011), or the upcoming DLR TanDEM-X GDEM (Zink et al., 2014), whose absolute elevation in some regions has been assessed to be within ±10 m. They will also need to be coupled with a coherent global water mask more precise than that of Globcover. For example, the global water mask established from satellite imagery computed by Pekel et al. (2016) could represent a good alternative. Some local information provided by the broader scientific community (based on field

trip measurements, local maps…) could also be used. For locations where an accurate on-board DEM over water bodies cannot be computed, the altimeter would be left in classical CL tracking mode, to avoid setting the tracking window to an incorrect position for all cycles. In the coming years, more extensive work will be needed to improve the Jason-3 on-board DEM, but also for incoming altimetry missions that are not on the same orbit (for example the Sentinel-3 series of satellites).

The benefits of the OL tracking mode for lakes and reservoirs need to be carefully investigated. Similar results are anticipated to those obtained for rivers where an accurate on-board DEM can be computed. However computation of the on-board DEM may be even harder than for rivers, as many reservoirs (and lakes) are in mountainous regions where the DEMs usually available are not accurate to within ±10 m. Further, for large lakes and reservoirs, the OL tracking mode might not be suitable, as they can display seasonal and/or interannual variations much larger than those of rivers. For such variations, setting the tracking window to one constant value might not be appropriate for all observation times. A potential solution would be to update the on-board DEM on a seasonal basis. Specific studies are needed to investigate these cases.

Acknowledgements:

Our warm thanks to IGN for freely providing numerous georeferenced information across France (DEM is available at http://professionnels.ign.fr/ and river network data at www.sandre.eaufrance.fr).

The authors are grateful to SCHAPI for making gage measurements from the many gages operated by different agencies in France publicly available, through the ‘Banque Hydro’ database (http://www.hydro.eaufrance.fr).

CEREMA (Vanessya LABORIE), DREAL Auvergne Rhône-Alpes (Eric KERMAREC and Philippe PRAX), DREAL Bourgogne-Franche-Comté (Erwan LE BARBU), DREAL Centre-Val de Loire (Franck GILLOUX), DREAL Grand Est (Christophe MAGE, Johan HABERT and Marc KLIPFEL), DREAL Nouvelle-Aquitaine (Olivier DEBINSKI et Dominique LAGORCE), DREAL Occitanie (Arthur MARCHANDISE et Didier NARBAÏS-JAUREGUY), and DREAL Pays de la Loire (Stéphanie POLIGOT-PITSCH) are also gratefully thanked for providing some in situ measurements and gage elevations used in this study.

CNES, NASA, EUMETSAT, NOAA, and Copernicus are acknowledged for providing free access for the scientific community to measurements from Jason-2 and Jason-3 altimeters.

The CTOH observation service at LEGOS (http://ctoh.legos.obs-mip.fr/) is also acknowledged for processing and providing altimetry data in a uniform format.

Constructive comments from Nicolas Picot (CNES) helped to improve this article.

This study was funded by the ‘‘Réseau Thématique de Recherche Avancée - Sciences et Technologies pour l’Aéronautique et l’Espace” (RTRA-STAE, Toulouse, France), through a grant awarded to the ‘‘Ressources en Eau sur le bassin de la GARonne: interaction entre les composantes naturelles et anthropiques et apport de la téléDétection” (REGARD) project.

This work was supported by the CNES. It is based on observations with Poseidon-3 and Poseidon-3B embarked on Jason-2 and Jason-3, respectively. Especially, funding from the CNES Terre-Océan-Surfaces Continentales-Athmosphère (TOSCA) committee to the “AltiWaveforms” and CTOH projects, and from the Ocean Surface Topography Science Team (OSTST) FOAM project is acknowledged.

Finally, comments and suggestions from three anonymous reviewers improved this article.

References:

Baup, F., Frappart, F., Maubant, J., 2014. Combining high-resolution satellite images and altimetry to estimate the volume of small lakes. Hydrol. Earth Syst. Sci. 18, 2007–2020. http://dx.doi.org/10.5194/hess-18-2007-2014.

Berry, P.A.M., Hilton, R., Johnson, C.P.D., Pinnock, R.A., 2000. ACE: a new GDEM incorporating satellite altimeter derived heights. In: Proceedings of the ERS-EnvisatSymposium, Gothenburg, Sweden, ESA SP-461, pp. 783–791.

Berry, P.A.M., Smith, R.G., Benveniste, J., 2010. ACE2: the new global digital elevation model. In: Mertikas, P.S. (Ed.), Gravity, Geoid and Earth Observation: IAG Commission 2: Gravity Field, Chania, Crete, Greece, 23–27 June 2008. Springer, Berlin-Heidelberg, pp. 231–237. http://dx.doi.org/10.1007/978-3-642-10634-7_30, ISBN: 978-3-642-10634-7.

Biancamaria, S., Frappart, F., Leleu, A.-S., Marieu, V., Blumstein, D., Desjonquères, J.-D., Boy, F., Sottolichio, A., Valle-Levinson, A., 2017. Satellite radar altimetry water elevations performance over a 200 m wide river: Evaluation over the Garonne River. Adv. Space Res. 59(1), 128-146. http://doi.org/10.1016/j.asr.2016.10.008.

Birkett, C.M., 1995. The contribution of TOPEX/POSEIDON to the global monitoring of climatically sensitive lakes. J. Geophys. Res.: Oceans 100, 25179–25204. http://dx.doi.org/10.1029/95JC02125.

Birkett, C.M., 1998. Contribution of the TOPEX NASA radar altimeter to the global monitoring of large rivers and wetlands. Water Resour. Res. 34 (5), 1223–1239. http://dx.doi.org/10.1029/98WR00124.

643 Birkett, C. M., Beckley, B., 2010. Investigating the Performance of the Jason-2/OSTM Radar
644 Altimeter over Lakes and Reservoirs. Marine Geodesy 33 (S1), 204-238.
645 http://dx.doi.org/10.1080/01490419.2010.488983.
646 Brown, G.S., 1977. The average impulse response of a rough surface and its application. IEEE
647 Trans. Antennas Propag. 67–74. http://dx.doi.org/10.1109/TAP.1977.1141536.
648 Chelton, D.B., Ries, J.C., Haines, B.J., Fu, L.-L., Callahan, P.S., 2001. Satellite altimetry. In: Fu,
649 L.-L., Cazenave, A. (Eds.), Satellite Altimetry and Earth Sciences. Academic Press, San
650 Diego, pp. 27–32.
651 Couhert, A., Cerri, L., Legeais, J.-F., Ablain, M., Zelensky, N.P., Haines, B.J., Lemoine, F.G.,
652 Bertiger, W.I., Desai, S.D., Otten, M., 2015. Towards the 1 mm/y stability of the radial
653 orbit error at regional scales. Adv. Space Res. 55(1), 2-23.
654 http://dx.doi.org/10.1016/j.asr.2014.06.041.
655 Crétaux, J.-F., Nielsen, K., Frappart, F., Papa, F., Calmant, S., Benveniste, J., 2017. Hydrological
656 applications of satellite altimetry: rivers, lakes, man-made reservoirs, inundated areas. In:
657 Stammer, D., Cazenave, A. (Eds.), Satellite Altimetry Over Oceans and Land Surfaces,
658 Earth Observation of Global Changes. CRC Press.
659 Desjonquères, J.D., 2009. POSEIDON3 DEM/Diode Coupling Mode. 2009 OSTST Meeting,
660 Seattle, USA.
661 http://www.aviso.altimetry.fr/fileadmin/documents/OSTST/2009/oral/Desjonqueres_coasta
662 l.pdf (accessed 12.04.17).
663 Desjonquères, J.-D., Carayon, G., Steunou, N., Lambin, J., 2010. Poseidon-3 radar altimeter:
664 new modes and in-flight performances. Mar. Geodesy 33 (S1), 53–79.
665 http://dx.doi.org/10.1080/01490419.2010.488970.

Dumont, J.-P., Rosmorduc, V., Carrère, L., Picot, N., Bronner, E., Couhert, A., Guillot, A., Desai, S., Bonekamp, H., Figa, J., Scharroo, R., Lillibridge, J., (2016). Jason-3 product handbook. Issue 1rev2. https://www.nodc.noaa.gov/media/pdf/jason2/j3_user_handbook.pdf (accessed 06.06.17).

Fekete, B. M., Looser, U., Pietroniro, A., Robarts, R. D., 2012. Rationale for monitoring discharge on the ground. J. Hydrometeor. 13, 1977-1986. http://dx.doi.org/10.1175/JHM-D-11-0126.1.

Frappart, F., Calmant, S., Cauhopé, M., Seyler, F., Cazenave, A., 2006. Preliminary results of ENVISAT RA-2 derived water levels validation over the Amazon basin. Rem. Sens. Environ. 100 (2), 252–264. http://dx.doi.org/10.1016/j.rse.2005.10.027.

Frappart, F., Papa, F., Malbeteau, Y., León, J.G., Ramillien, G., Prigent, C., Seoane, L., Seyler, F., Calmant, S., 2015a. Surface freshwater storage variations in the Orinoco floodplains using multi-satellite observations. Rem. Sens. 7 (1), 89–110. http://dx.doi.org/10.3390/rs70100089.

Frappart, F., Papa, F., Marieu, V., Malbeteau, Y., Jordy, F., Calmant, S., Durand, F., Bala, S., 2015b. Preliminary assessment of SARAL/AltiKa observations over the Ganges-Brahmaputra and Irrawaddy Rivers. Mar. Geodesy. 38 (sup1), 568–580. http://dx.doi.org/10.1080/01490419.2014.990591.

Frappart, F., Fatras, C., Mougin, E., Marieu, V., Diepkile, A.T., Blarel, F., Borderies, P., 2015c. Radar altimetry backscattering signatures at Ka, Ku, C and S bands over West Africa. Phys. Chem. Earth Pt. A/B/C 83-84, 96-110. http://dx.doi.org/10.1016/j.pce.2015.05.001.

Frappart, F., Blumstein, D., Cazenave, A., Ramillien, G., Birol, F., Morrow, R., Rémy, F., 2017. Satellite altimetry: principle and major applications in Earth Sciences. In: Webster, J. (Ed.),

689 Wiley Encyclopedia of Electrical and Electronics Engineering. John Wiley & Sons Inc.,
690 pp. 1-25. http://dx.doi.org/10.1002/047134608X.W1125.pub2.
691 Fu, L.-L., Cazenave, A., 2001. Satellite Altimetry and Earth Sciences. Academic Press, San
692 Diego, ISBN:0-12-269545-3,2.
693 Gleason, C. J., Hamdan, A. N., 2017. Crossing the (watershed) divide: satellite data and the
694 changing politics of international river basins. The Geogr. J. 183 (1), 2-15.
695 http://dx.doi.org/10.1111/geoj.12155.
696 IGN, 2017. BD Alti version 2.0. http://professionnels.ign.fr/sites/default/files/DC_BDALTI_2-
697 0.pdf (accessed 16.04.17).
698 International Association of Hydrological Sciences (IAHS) Ad Hoc Group on Global Water Data
699 Sets, Vörösmarty, C., Askew, A., Grabs, W., Barry, R. G., Birkett, C., Döll, P., Goodison,
700 B., Hall, A., Jenne, R., Kitaev, L., Landwehr, J., Keeler, M., Leavesley, G., Schaake, J.,
701 Strzepek, K., Sundarvel, S. S., Takeuchi, K., Webster, F., 2001. Global water data: A newly
702 endangered species. Eos Trans. AGU 82 (5), 54–58. http://dx.doi.org/10.1029/01EO00031.
703 Koblinsky, C. J., Clarke, R. T., Brenner, A. C., Frey, H., 1993. Measurement of river level
704 variations with satellite altimetry. Water Resour. Res. 29(6), 1839-1848.
705 http://dx.doi.org/10.1029/93WR00542.
706 Michailovsky, C.I., McEnnis, S., Berry, P.A.M., Smith, R., Bauer-Gottwein, P., 2012. River
707 monitoring from satellite radar altimetry in the Zambezi River basin. Hydrol. Earth Syst.
708 Sci. 16, 2181–2192. http://dx.doi.org/10.5194/hess-16-2181-2012.
709 Moriasi, D.N. , Arnold, J.G., Van Liew, M.W., Bingne, R.L., Harmel, R.D., Veith, T.L.. 2007.
710 Model evaluation guidelines for systematic quantification of accuracy in watershed
711 simulations. Trans. ASABE 50 (3), 885–900.

712 Nash, J.E., Sutcliffe, J.V., 1970. River flow forecasting through conceptual models Part I – A
713 discussion of principles. J. Hydrol. 10 (3), 282–290. http://dx.doi.org/10.1016/0022-
714 1694(70)90255-6.
715 Pekel, J.-F., Cottam, A., Gorelick, N., Belward, A. S., 2016. High-resolution mapping of global
716 surface water and its long-term changes. Nature, 540, 418-422. http://dx.doi.org/
717 10.1038/nature20584.
718 Santos da Silva, J., Calmant, S., Seyler, F., Corrêa Rotunno Filho, O., Cochonneau, G., Mansur,
719 W.J., 2010. Water levels in the Amazon basin derived from the ERS 2 and ENVISAT radar
720 altimetry missions. Rem. Sens. Environ. 114, 2160–2181.
721 http://dx.doi.org/10.1016/j.rse.2010.04.020.
722 Stöckli, R., Vermote, E., Saleous, N., Simmon, R., Herring, D., 2005. The Blue Marble Next
723 Generation - A true color earth dataset including seasonal dynamics from MODIS.
724 Published by the NASA Earth Observatory.
725 https://earthobservatory.nasa.gov/Features/BlueMarble/ (accessed 25.04.17).
726 Sulistioadi, Y.B., Tseng, K.-H., Shum, C.K., Hidayat, H., Sumaryono, M., Suhardiman, A.,
727 Setiawan, F., Sunarso, S., 2015. Satellite radar altimetry for monitoring small rivers and
728 lakes in Indonesia. Hydrol. Earth Syst. Sci. 19, 341–359. http://dx.doi.org/10.5194/hess-
729 19-341-2015.
730 Tachikawa, T., Hato, M., Kaku, M., Iwasaki, A., 2011. Characteristics of ASTER GDEM version
731 2. International Geoscience and Remote Sensing Symposium (IGARSS) 2011, Vancouver,
732 Canada.
733 Tapley, B., Ries, J., Bettadpur, S., Chambers, D., Cheng, M., Condi, F., Gunter, B., Kang, Z.,
734 Nagel, P., Pastor, R., Pekker, T., Poole, S., Wang, F., 2005. GGM02 - An improved Earth

gravity field model from GRACE. J. Geodesy 79 (8), 467-478. http://dx.doi.org/10.1007/s00190-005-0480-z.

Wingham, D.J., Rapley, C.G., Griffiths, H., 1986. New techniques in satellite altimeter tracking systems. In: ESA (Ed.), Proceedings of IGARSS'86 Symposium, Zürich, 8–11 September 1986, SP-254, 1339–1344.

Zink, M., Bachmann, M., Bräutigam, B., Fritz, T., Hajnsek, I., Moreira, A., Wessel, B., Krieger, G., 2014. TanDEM-X: the new global DEM takes shape. IEEE Geosci. Rem. Sens. Mag. 2 (2), 8-23. http://dx.doi.org/10.1109/MGRS.2014.2318895.

List of figure captions:

Figure 1. Conceptual view of nadir altimeter measurements and notations used in this study (the copyright of the Jason-3 satellite image used in this sketch belongs to CNES/Mira Production)

Figure 2. Study domain (Mainland France, delimited by the black line) and the river network (light blue lines) from the IGN BD Carthage database (only rivers wider than 50 m according to this database are shown). Red lines correspond to Jason-2 and Jason-3 tandem phase orbit tracks. White and red diamonds correspond to virtual stations (VS), where Jason-3 on-board DEM values were computed. Red diamonds are virtual stations where Jason-2 and Jason-3 river elevation time series were compared to in situ gage (green stars) measurements. The background image is derived from the NASA MODIS "Blue Marble Next Generation" image (Stöckli et al., 2005)

Figure 3. Mean absolute difference (dR) between Rtrack and RDEM (see Figure 1) for Jason-2 (a. and b.) and Jason-3 (c. and d.) for cycles when Jason-3 is in closed-loop mode (approximately between February and May, 2016; a. and c.) and when Jason-3 is in open-loop mode (approximately between May and September, 2016, see Table 1 for the list of cycles; b. and d.)

Figure 4. Jason-2 (left panels; a., c. and e.) and Jason-3 (right panels; b., d. and f.) water elevation time series (red lines and red dots) on the Loire River at La Menitré (JA-082) compared to in situ time series (blue lines and blue dots) at Gennes. Top panels (a. and b.) correspond to absolute elevations with reference to (wrt) NGF-IGN69 at satellite observation times. Middle panels (c. and d.) correspond to elevation anomalies at satellite observation times. Bottom panels (e. and f.) correspond to times series with all available times for both satellite and in situ time series. Pale rose zones on panels b., d., and f. correspond to time periods when Jason-3 altimeter was in CL tracking mode

Figure 5. Jason-2 (left panels; a., c. and e.) and Jason-3 (right panels; b., d. and f.) water elevation time series (red lines and red dots) on the Garonne River at Caumont-sur-Garonne (JA-030) compared to in situ time series (blue lines and blue dots) at Tonneins. Panels are similar to those in Figure 4. Pale rose zones on panels b., d., and f. correspond to time periods when Jason-3 altimeter was in CL tracking mode

Figure 6. Jason-2 (left panels; a., c. and e.) and Jason-3 (right panels; b., d. and f.) water elevation time series (red lines and red dots) on the Loire River at Saint-Michel-sur-Loire (JA-064) compared to in situ time series (blue lines and blue dots) at Langeais. Panels are similar to

those in Figure 4. As Jason-2 is locked on the surrounding topography, panels c. and e. are not relevant, but are kept for consistency with Figure 4 and Figure 5. Pale rose zones on panels b., d., and f. correspond to time periods when Jason-3 altimeter was in CL tracking mode